



The Probability of Extinction of Infectious Salmon Anemia Virus in One and Two Patches

Evan Milliken¹ 

Received: 14 November 2016 / Accepted: 27 September 2017
© Society for Mathematical Biology 2017

1 **Abstract** Single-type and multitype branching processes have been used to study the
2 dynamics of a variety of stochastic birth–death type phenomena in biology and physics.
3 Their use in epidemiology goes back to Whittle’s study of a susceptible–infected–
4 recovered (SIR) model in the 1950s. In the case of an SIR model, the presence of only
5 one infectious class allows for the use of single-type branching processes. Multitype
6 branching processes allow for multiple infectious classes and have latterly been used
7 to study metapopulation models of disease. In this article, we develop a continuous
8 time Markov chain (CTMC) model of infectious salmon anemia virus in two patches,
9 two CTMC models in one patch and companion multitype branching process (MTBP)
10 models. The CTMC models are related to deterministic models which inform the
11 choice of parameters. The probability of extinction is computed for the CTMC via
12 numerical methods and approximated by the MTBP in the supercritical regime. The
13 stochastic models are treated as toy models, and the parameter choices are made to
14 highlight regions of the parameter space where CTMC and MTBP agree or disagree,
15 without regard to biological significance. Partial extinction events are defined and their
16 relevance discussed. A case is made for calculating the probability of such events,
17 noting that MTBPs are not suitable for making these calculations.

1

2

3

18 **Keywords** Multitype branching process · Probability of extinction

✉ Evan Milliken
emilliken@gmail.com

¹ School of Mathematical and Statistical Sciences, Arizona State University, Tempe, Arizona, USA

19 **1 Introduction**

20 In the investigation that follows, we will use the case of an outbreak of infectious
 21 salmon anemia (ISA) as a test case to examine some of the features of MTBP approx-
 22 imation of a CTMC. Infectious salmon anemia virus (ISAv) causes (ISA) which leads
 23 to 15–100% accumulated mortality over the course of a several-month-long infection
 24 in a farm environment (Falk et al. 1997). It is found in all large salmon-producing
 25 countries including Norway, Scotland, Ireland, Canada, the USA, and Chile (Vike
 26 et al. 2009). ISAv is transmitted among finfish horizontally by passive movement of
 27 infected seawater (Mardones et al. 2009) and via direct contact with excretions or
 28 secretions of infected individuals. Salmon farms consist of a collection of net cages
 29 placed in open body of water. This array-like structure of a farm and the proxim-
 30 ity of farms to each other and to wild salmon migratory routes justifies the use of a
 31 metapopulation approach.

32 Branching processes have been used to study a variety of biological phenomena
 33 dating back to their invention to answer a question regarding the extinction of aristo-
 34 cratic surnames. Bienaymé made the first contribution in 1845 (Seneta 1998) before
 35 the question was made well known by Galton and answered together with Watson in
 36 1873–1874 (Watson and Galton 1875). As a result, the class of single-type branch-
 37 ing processes came to be known as Bienaymé–Galton–Watson branching processes
 38 (BGWbp). A special case considering two types of individuals was studied by Bartlett
 39 in 1946, and BGWbp theory was extended to include general multitype branching
 40 processes by Kolmogorov, Dmitriev, Sevastyanov, Everett, and Ulam in the late 1940s
 41 (Harris 1963). BGWbp and MTBP models have been used to study a variety of phe-
 42 nomena in biology and physics including population dynamics, changes to the genome,
 43 cell kinetics, cancer, and epidemiology (Allen 2003; Allen and Lahodny 2012, 2013;
 44 Allen and Driessche 2013; Ball 1983; Ball and Donnelly 1995; Britton 2010; Dorman
 45 et al. 2004; Griffiths and Greenhalgh 2011; Harris 1963; Kimmel and Axelrod 2002;
 46 Whittle 1955). In particular, Allen and Lahodny studied MTBPs as an approximation
 47 of the outbreak dynamics of a CTMC model of infection in single- and multipatch
 48 models (Allen and Lahodny 2012, 2013).

49 We recall earlier analysis of deterministic susceptible–infected–virus (SIV) models
 50 of ISAv outbreak in one and two patches to inform our investigation and aid in suitable
 51 parameter selection (Milliken 2016). The model in one patch is adapted from well-
 52 studied models (Beretta and Kuang 1998; Nowak and May 2000; Perelson and Nelson
 53 1999) by allowing for direct transmission via contact with infected individuals. For
 54 each of these two models, a companion CTMC model is introduced, as well as a
 55 MTBP. The probability of extinction of the disease is approximated for the CTMC
 56 using numerical simulation. Approximation is also made via the analysis of the MTBP,
 57 and the results are compared with those of numerical simulation.

58 Formulation of a birth–death process as a branching process relies on the fact that
 59 all transitions are independent (Allen and Lahodny 2012; Harris 1963; Mode 1971).
 60 This is a strong biological assumption, but one commonly made for the purpose of
 61 mathematical modeling. In order to formulate epidemiological models as branching
 62 processes, an additional assumption is made: the susceptible population remains fixed
 63 at its initial (disease-free) population size. As a result of this assumption, MTBP only

64 provides accurate approximation of the probability of disease extinction when the total
 65 population size is sufficiently large. There is currently no analytic estimate for how
 66 large is sufficiently large. In order to illustrate the breakdown of MTBP approximation
 67 and explore its dependence on the underlying system and its parameters, we calculate
 68 the probability of extinction for a one-patch system for a range of initial population
 69 sizes at two different levels of infected fish mortality. We also propose a variation
 70 on the deterministic one-patch model by changing the assumed force of infection
 71 (f.o.i.). Corresponding CTMC and MTBP models are also developed. The probability
 72 of extinction is again calculated at various initial population sizes.

73 MTBP techniques are suitable to calculate the probability of complete extinction
 74 of the disease in all forms and in all patches. A partial extinction event is one in which
 75 one or more classes of infectious individuals goes extinct, but at least some class
 76 remains endemic. Such events are transient from the prospective of deterministic and
 77 stochastic modeling and have not been considered to date. Metapopulation models are
 78 characterized by multiple patches and the rates of movement between them. It is of
 79 particular interest to consider partial extinction events in a metapopulation in which
 80 the disease goes extinct in some, but not all patches. Statistics like the probability of
 81 partial extinction events may help to understand how the underlying structure of the
 82 metapopulation influences the dynamics of the system. Additionally, the probability of
 83 extinction in a single patch of a metapopulation model may be viewed as a numerical
 84 rating of how susceptible that patch is to outbreak of disease. When a patch corresponds
 85 to a locality, this rating could then be used to optimize control strategies from the
 86 perspective of that patch. An attempt to study partial extinction events for an outbreak
 87 of ISA_v in two patches using MTBP techniques led to the determination that these
 88 techniques are not suitable to answer such questions.

89 2 Two-Patch Model of ISA_v

90 We begin by illustrating the use of MTBP to approximate the probability of extinction
 91 in metapopulation models by taking a two-patch model of ISA_v as a test case. The
 92 CTMC is constructed so that it is related to a previously studied deterministic model
 93 (Milliken 2016). As a result, the quasi-steady state is equal to the endemic equilibrium
 94 of the deterministic model. Parameters are chosen to ensure the quasi-steady state
 95 associated with outbreak exists and can be easily located numerically. They are also
 96 chosen to ensure the accuracy of the MTBP approximation. They are not chosen for
 97 biological relevance.

98 2.1 Deterministic SIV–SIV Model

99 In previous work with Milliken (2016), we proposed a two-patch SIV model to study
 100 the dynamics of an ISA_v infection. The two patches are coupled solely via diffusion
 101 of the virus. Birth and death rates are patch dependent and are denoted by a subscript
 102 associated with the patch. All other parameters are patch independent. The force of
 103 infection in the i th patch is given by $S_i(\sigma I_i + \rho V_i)$, but the parameters σ and ρ can
 104 be scaled away. Rescaling yields the following system:

$$\begin{cases}
 \dot{S}_1 = S_1(\beta_1 - \mu_1 S_1) - S_1(I_1 + V_1) \\
 \dot{I}_1 = S_1(I_1 + V_1) - \alpha I_1 \\
 \dot{V}_1 = k(V_2 - V_1) - \omega V_1 + \delta I_1 \\
 \dot{S}_2 = S_2(\beta_2 - \mu_2 S_2) - S_2(I_2 + V_2) \\
 \dot{I}_2 = S_2(I_2 + V_2) - \alpha I_2 \\
 \dot{V}_2 = k(V_1 - V_2) - \omega V_2 + \delta I_2.
 \end{cases} \quad (1)$$

where β_1, β_2 are the patch-specific birth rates of susceptible fish, μ_1, μ_2 are the patch-specific, density-dependent mortality rates, α is the mortality rate of infected fish, δ is the rate at which infected fish shed the virus into the environment, ω is the rate at which it clears from the environment, and k is the rate of viral diffusion.

System (1) admits 7 equilibria in total. Four equilibria corresponding to the absence of the virus: $(0,0,0,0,0,0)$, $(\bar{S}_1, 0, 0, 0, 0, 0)$, $(0, 0, 0, \bar{S}_2, 0, 0)$, DFE = $(\bar{S}_1, 0, 0, \bar{S}_2, 0, 0)$. Of these, only the disease-free equilibrium (DFE) is locally stable in the subspace associated with the absence of the disease. Let

$$\mathcal{R}_0^{(1)} = \frac{(\omega(2k + \omega) + \delta(k + \omega))\beta_1}{\alpha\omega(2k + \omega)\mu_1} \quad \mathcal{R}_0^{(2)} = \frac{(\omega(2k + \omega) + \delta(k + \omega))\beta_2}{\alpha\omega(2k + \omega)\mu_2}.$$

Then $\mathcal{R}_0^{(i)}$ is the patch-specific reproduction numbers corresponding to host fish only in patch i . System (1) admits two additional equilibria corresponding to the case where there are host fish only in patch one or only in patch two: $(S'_1, I'_1, V'_1, 0, 0, V'_2) \iff \mathcal{R}_1^0 > 1$ and $(0, 0, V_1^*, S_2^*, I_2^* V_2^*) \iff \mathcal{R}_2^0 > 1$. The basic reproduction number for system (1) is given by

$$\mathcal{R}_0 = \frac{1}{2} \left(\mathcal{R}_1^0 + \mathcal{R}_2^0 + \sqrt{(\mathcal{R}_1^0 - \mathcal{R}_2^0)^2 + 4\bar{S}_1\bar{S}_2C^2} \right),$$

where $C = \frac{\delta k}{\alpha\omega(2k + \omega)}$. Following Milliken (2016), we have that DFE is globally asymptotically stable (g.a.s.) if and only if $\mathcal{R}_0 \leq 1$. If $\mathcal{R}_0 > 1$, then the DFE is unstable and the virus invades and persists when introduced. In fact, the subset of the boundary associated with the extinction of the virus is a uniform strong repeller whenever $\mathcal{R}_0 > 1$ (Butler et al. 1986; Fonda 1988; Freedman et al. 1994; Garay 1989; Hofbauer and So 1989; Milliken 2016; Thieme 1993). If, in addition, the following symmetric conditions are met,

$$\mathcal{R}_1^0 > \frac{\mu_2}{\mu_1} Q(\mathcal{R}_2^0 - 1) \quad \text{and} \quad \mathcal{R}_2^0 > \frac{\mu_1}{\mu_2} Q(\mathcal{R}_1^0 - 1),$$

where $Q = \frac{\delta k}{\omega(2k + \omega) + \delta(k + \omega)}$, then there exists a unique positive endemic equilibrium.

Table 1 State transitions and rates for the two-patch CTMC model, X_t

Description	Transition	Rate $\sigma(i, j)$
Birth of S_1	$(S_1, I_1, V_1, S_2, I_2, V_2) \mapsto (S_1 + 1, I_1, V_1, S_2, I_2, V_2)$	$\beta_1 S_1$
Death of S_1	$(S_1, I_1, V_1, S_2, I_2, V_2) \mapsto (S_1 - 1, I_1, V_1, S_2, I_2, V_2)$	$\mu_1 S_1^2$
Infection of S_1	$(S_1, I_1, V_1, S_2, I_2, V_2) \mapsto (S_1 - 1, I_1 + 1, V_1, S_2, I_2, V_2)$	$S_1(I_1 + V_1)$
Death of I_1	$(S_1, I_1, V_1, S_2, I_2, V_2) \mapsto (S_1, I_1 - 1, V_1, S_2, I_2, V_2)$	αI_1
Shedding of V_1	$(S_1, I_1, V_1, S_2, I_2, V_2) \mapsto (S_1, I_1, V_1 + 1, S_2, I_2, V_2)$	δI_1
Clearance of V_1	$(S_1, I_1, V_1, S_2, I_2, V_2) \mapsto (S_1, I_1, V_1 - 1, S_2, I_2, V_2)$	ωV_1
Diffusion of V_1	$(S_1, I_1, V_1, S_2, I_2, V_2) \mapsto (S_1, I_1, V_1 - 1, S_2, I_2, V_2 + 1)$	$k V_1$
Birth of S_2	$(S_1, I_1, V_1, S_2, I_2, V_2) \mapsto (S_1, I_1, V_1, S_2 + 1, I_2, V_2)$	$\beta_2 S_2$
Death of S_2	$(S_1, I_1, V_1, S_2, I_2, V_2) \mapsto (S_1, I_1, V_1, S_2 - 1, I_2, V_2)$	$\mu_2 S_2^2$
Infection of S_2	$(S_1, I_1, V_1, S_2, I_2, V_2) \mapsto (S_1, I_1, V_1, S_2 - 1, I_2 + 1, V_2)$	$S_2(I_2 + V_2)$
Death of I_2	$(S_1, I_1, V_1, S_2, I_2, V_2) \mapsto (S_1, I_1, V_1, S_2, I_2 - 1, V_2)$	αI_2
Shedding of V_2	$(S_1, I_1, V_1, S_2, I_2, V_2) \mapsto (S_1, I_1, V_1, S_2, I_2, V_2 + 1)$	δI_2
Clearance of V_2	$(S_1, I_1, V_1, S_2, I_2, V_2) \mapsto (S_1, I_1, V_1, S_2, I_2, V_2 - 1)$	ωV_2
Diffusion of V_2	$(S_1, I_1, V_1, S_2, I_2, V_2) \mapsto (S_1, I_1, V_1 + 1, S_2, I_2, V_2 - 1)$	$k V_2$

130 **2.2 Stochastic SIV–SIV Model**

131 From the preceding deterministic model, we construct the CTMC, $\mathbf{X}(t) = (S_1(t),$
 132 $I_1(t), V_1(t), S_2(t), I_2(t), V_2(t))$, with the infinitesimal transition probability to state
 133 j from state i given by

134
$$p_{i,j}(\Delta t) = \mathbb{P}\{\mathbf{X}(t + \Delta t) = j \mid \mathbf{X}(t) = i\} = \sigma(i, j)\Delta t + o(\Delta t),$$

135 where $\sigma(i, j)$ is the rate associated with the transition from state i to state j and can
 136 be found in Table 1.

137 *Remark 1* Recall that the original force of infection in the i th patch given by $S_i(\sigma I_i +$
 138 $\rho V_i)$. S and V are rescaled and μ and δ relabeled yielding (1) for easier analysis. The
 139 V that is retained represents a scalar multiple of the number of virions present. Let μ
 140 and δ reflect $\sigma = 1$ and ρ chosen so that we may interpret 1 unit of V as any number of
 141 virions, such as an average infectious viral dose (e.g., ID50). This makes the transition
 142 $V \mapsto V + 1$ in the rescaled model reasonable.

143 We are interested in studying the dynamics after infectious agents are introduced
 144 to an entirely susceptible system. Analysis of the flow of (1) on the boundary shows
 145 that, in the absence of the disease, DFE is g.a.s.. Therefore, we assume that DFE is
 146 the initial state of the system prior to introduction of the disease. As X_t evolves in
 147 time, $S_1(t)$ and $S_2(t)$ evolve along with all the other state components. To formulate
 148 the MTBP, we first pass to embedded discrete time Markov chain (DTMC), X_n . Next,
 149 suppose that $S_1(n) \equiv \bar{S}_1$ and $S_2(n) \equiv \bar{S}_2$, the disease-free populations of susceptible
 150 fish in patches 1 and 2, respectively, and that each individual gives birth independently
 151 of other individuals. Let $Z_n = (I_1(n), V_1(n), I_2(n), V_2(n))$ be the random variable

152 associated with the n th generation. The offspring probability generating function (pgf)
153 is given by

$$154 \quad \mathbf{F}(\mathbf{u}) = (f_1(\mathbf{u}), f_2(\mathbf{u}), f_3(\mathbf{u}), f_4(\mathbf{u})),$$

155 where, for $i = 1, 2, 3, 4$,

$$156 \quad f_i((u_1, u_2, u_3, u_4)) = \sum_{n=0}^{\infty} p_i(r_1, \dots, r_4) u_1^{r_1} \dots u_4^{r_4},$$

157 and $p_i(r_1, \dots, r_4)$ is the probability that an object of type i gives birth to r_1 offspring
158 of type 1, \dots , and r_4 offspring of type 4. The offspring pgf for I_1 is

$$159 \quad f_1(\mathbf{u}) = \frac{\alpha + \delta u_1 u_2 + \bar{S}_1 u_1^2}{\alpha + \delta + \bar{S}_1},$$

160 the offspring pgf for V_1 is

$$161 \quad f_2(\mathbf{u}) = \frac{\omega + k u_4 + \bar{S}_1 u_1 u_2}{\omega + k + \bar{S}_1},$$

162 the offspring pgf for I_2 is

$$163 \quad f_3(\mathbf{u}) = \frac{\alpha + \delta u_3 u_4 + \bar{S}_2 u_3^2}{\alpha + \delta + \bar{S}_2},$$

164 and the offspring pgf for V_2 is

$$165 \quad f_4(\mathbf{u}) = \frac{\omega + k u_2 + \bar{S}_2 u_3 u_4}{\omega + k + \bar{S}_2}.$$

166 The matrix of expectations $\mathbb{M} = D\mathbf{F}(\mathbf{1})$ is given by

$$167 \quad \mathbb{M} = \begin{bmatrix} \frac{\delta + 2\bar{S}_1}{\alpha + \delta + \bar{S}_1} & \frac{\delta}{\alpha + \delta + \bar{S}_1} & 0 & 0 \\ \frac{\bar{S}_1}{\omega + k + \bar{S}_1} & \frac{\bar{S}_1}{\omega + k + \bar{S}_1} & 0 & \frac{k}{\omega + k + \bar{S}_1} \\ 0 & 0 & \frac{\delta + 2\bar{S}_2}{\alpha + \delta + \bar{S}_2} & \frac{\delta}{\alpha + \delta + \bar{S}_2} \\ 0 & \frac{k}{\omega + k + \bar{S}_2} & \frac{\bar{S}_2}{\omega + k + \bar{S}_2} & \frac{\bar{S}_2}{\omega + k + \bar{S}_2} \end{bmatrix}.$$

168 A branching process is called positively regular if \mathbb{M} is primitive. A k -many type
169 process is called not singular if $F(\mathbf{0}) > \mathbf{0}$ with respect to the standard order, and
170 whenever $\mathbf{x}, \mathbf{y} \in [0, 1]^k$ with $\mathbf{x} \leq \mathbf{y}$, then $D\mathbf{F}(\mathbf{x}) \leq D\mathbf{F}(\mathbf{y})$. The i, j th entry of $D\mathbf{F}(\mathbf{1})$
171 is $\frac{\partial f_i}{\partial u_j}(\mathbf{1})$, the expected number of type j offspring of an individual of type i . Following
172 Harris (1963), let q_i be the extinction probability if initially there is one object of type
173 $i, i = 1, \dots, k$. Let $\mathbf{q} = (q_1, \dots, q_k)$. Let \mathbb{P}_0 be the probability of extinction of
174 the branching process given that $Z_0 = (j_1, \dots, j_k)$. Since we have assumed that
175 individuals give birth independent of one another,

$$\mathbb{P}_0 = q_1^{j_1} q_2^{j_2} \dots q_k^{j_k}.$$

The branching process constructed above to approximate ISAv in two patches is positively regular (in fact, $\mathbb{M}^3 > 0$). It is easily verified that it is also not singular. The threshold theorem of Allen and Driessche (2013) and Theorem 7.1 of Harris (1963) combine to give the following result.

Theorem 1 Suppose Z_n is a MTBP with probability generating function $\mathbf{F} : \mathbb{R}^k \rightarrow \mathbb{R}^k$ such that $\mathbf{F}(\mathbf{0}) > \mathbf{0}$, $D\mathbf{F}(\mathbf{x}) \leq D\mathbf{F}(\mathbf{y})$ whenever $\mathbf{x}, \mathbf{y} \in [0, 1]^k$ with $\mathbf{x} \leq \mathbf{y}$, and $D\mathbf{F}(\mathbf{1})$ is primitive. If $\mathcal{R}_0 \leq 1$, then $\mathbf{q} = \mathbf{1}$. If $\mathcal{R}_0 > 1$, then \mathbf{q} is the unique vector $\mathbf{0} \leq \mathbf{q} < \mathbf{1}$ satisfying $\mathbf{F}(\mathbf{q}) = \mathbf{q}$.

Remark 2 For a fixed initial vector z_0 , the probability of extinction $\mathbb{P}_0 = P(Z_n = \mathbf{0} | Z_0 = z_0 \text{ for some } n > 0)$. In a metapopulation model, the probability of extinction is, therefore, the probability that all infectious classes go extinct, in all patches. If we wanted to use MTBP approximation to calculate a partial extinction event, like extinction in one patch, we would have to recast the MTBP to only track the evolution of those infectious classes and assume the number of individuals in other infectious classes remains fixed. However, we already assumed that there are few individuals initially present in each infectious class. As we have discussed above, in order to justify the assumption that the number of individuals in a given class remains fixed, the initial population in that class must be sufficiently large. The MTBP is, therefore, not the appropriate tool to study partial extinction events.

2.3 Numerical Example

In order to illustrate the accuracy of MTBP approximation of the probability of total extinction in a metapopulation model, we choose parameter values according to two criteria: (i) the disease-free number of susceptible fish is sufficiently large in each patch for approximation by branching process; and (ii) the endemic equilibrium of the deterministic system (1) can be located numerically. The endemic equilibrium of (1) is a quasi-steady state of the CTMC and the embedded DTMC. The second criterion also implies that $\mathcal{R}_0 > 1$. Therefore, purely for the purpose of illustration and without regard to biological relevance, we consider the parameter vector $(\beta_1 = 4, \mu_1 = 0.05, \beta_2 = 2.4, \mu_2 = 0.04, \alpha = 3.3, \delta = 1.3, \omega = 4, k = 3)$. Then $\bar{S}_1 = 80$, $\bar{S}_2 = 60$, $\mathcal{R}_1^0 \approx 30$, $\mathcal{R}_2^0 \approx 22$, and $\mathcal{R}_0 \approx 30 \gg 1$. Recall that $\mathbb{P}_0 = q_1^{j_1} q_2^{j_2} q_3^{j_3} q_4^{j_4}$, where $Z_0 = (j_1, j_2, j_3, j_4)$ and q_i is the extinction probability if there is initial one object of type i . Because of this and due to the computational expense of simulating this model, we only consider initial states with one object of type $i, i = 1, \dots, 4$. The vector \mathbf{q} of extinction probabilities is determined by iterating the pgf from the initial vector $\mathbf{0}$. Let $\mathbb{P}_0^{(n)}$ denote the probability of extinction approximated by numerical simulation over n realizations. The results are presented in Table 2.

By the law of large numbers, as the number of realizations, n , increases to infinity, $\mathbb{P}_0^{(n)}$ tends to the true probability of extinction. Assuming that $\mathbb{P}_0^{(n)}$ is distributed normally, the error in approximating \mathbb{P}_0 with $\mathbb{P}_0^{(n)}$ goes to zero like $\frac{1}{\sqrt{n}}$. This implies that

Table 2 Probability of extinction of the virus from the initial state $(\bar{S}_1, I_1(0), V_1(0), \bar{S}_2, I_2(0), V_2(0))$ and parameter vector $(\beta_1 = 4, \mu_1 = 0.05, \beta_2 = 10, \mu_2 = 0.04, \alpha = 3.3, \delta = 1.3, \omega = 4, k = 3)$ is approximated by MTBP and numerically over 1,000,000 realizations

$I_1(0)$	$V_1(0)$	$I_2(0)$	$V_2(0)$	\mathbb{P}_0	$\mathbb{P}_0^{(1,000,000)}$
1	0	0	0	0.0406	0.0410
0	1	0	0	0.0501	0.0501
0	0	1	0	0.0538	0.0542
0	0	0	1	0.0650	0.0652

approximation of \mathbb{P}_0 to three decimal places by numerical simulation requires making 10^6 realizations, at great computational expense.

The results in Table 2 suggest that the MTBP approximates the probability of extinction in the CTMC very accurately. In this case, we were not able to solve the nonlinear system of equations given by $\mathbf{F}(\mathbf{q}) = \mathbf{q}$ for an analytical solution to the MTBP. However, we are able to approximate \mathbf{q} by iteration with little computational expense, since $\mathbf{F}^n(\mathbf{0}) \rightarrow \mathbf{q}$.

3 One-Patch Model

As discussed above, we must assume the number of susceptible individuals remains fixed at the disease-free level in order to utilize branching process techniques for SIV models. The disease-free population size must be at least as large as some critical value in order for this assumption to be reasonable. Currently, there is no analytic estimate of this critical size. In Sect. 5, we compare MTBP approximation and simulation of the CTMC at a range of small initial populations for two models. These models are introduced in this section and the next. The first is an invariant subsystem of (1), which models the dynamics of infection in a single patch. We consider this one-patch model because it reduces the computational expense while still retaining the key features of interest.

3.1 Deterministic SIV Model

When there is no diffusion, i.e., $k = 0$, then each patch of the two-patch system forms an invariant SIV subsystem given by:

$$\begin{cases} \dot{S} = S(\beta - \mu S) - Sf(I, V) \\ \dot{I} = Sf(I, V) - \alpha I \\ \dot{V} = -\omega V + \delta I. \end{cases} \quad (2)$$

where $f(I, V) = f_1(I, V) = (I + V)$, β is the birth rate of susceptible fish, μ the mortality rate of susceptible fish, α the mortality rate of infected fish, ω is the rate of

Table 3 State transitions and rates for the CTMC SIV model

Description	Transition	Rate $\sigma(i, j)$
Birth of S	$(S, I, V) \mapsto (S + 1, I, V)$	βS
Death of S	$(S, I, V) \mapsto (S - 1, I, V)$	μS^2
Infection	$(S, I, V) \mapsto (S - 1, I + 1, V)$	$S(I + V)$
Death of I	$(S, I, V) \mapsto (S, I - 1, V)$	αI
Shedding of V	$(S, I, V) \mapsto (S, I, V + 1)$	δI
Clearance of V	$(S, I, V) \mapsto (S, I, V - 1)$	ωV

240 viral clearing and δ is the rate of viral shedding. All of these parameters are assumed
 241 to be positive.

242 The system admits equilibria $(0,0,0)$ (which is always unstable) and the disease-free
 243 equilibrium (DFE), $(\bar{S},0,0)$. The basic reproduction number is,

$$244 \quad \mathcal{R}_0 = \frac{(\delta + \omega)\beta}{\alpha\omega\mu}. \tag{3}$$

245 when $\mathcal{R}_0 > 1$ the system also admits a unique positive endemic equilibrium. $\mathcal{R}_0 = 1$
 246 is also a threshold for the dynamics of the system. If $\mathcal{R}_0 \leq 1$, then the DFE is g.a.s.. If
 247 $\mathcal{R}_0 > 1$, then the DFE is unstable and the virus invades and persists when introduced.
 248 The largest invariant subset of the boundary is a uniform strong repeller when $\mathcal{R}_0 > 1$
 249 (Milliken 2016; Thieme 1993).

250 3.2 Stochastic SIV Model

251 The CTMC model $\mathbf{X}(t) = (S(t), I(t), V(t))$ associated with system (2) with
 252 $f(I, V) = f_1(I, V)$ is characterized by the transition rates given in Table 3.

253 To estimate the probability of extinction of the virus, we approximate the CTMC
 254 near the DFE (Fig. 1). As in the two-patch case, we pass to the embedded DTMC,
 255 assume that $S(n) \equiv \bar{S}$ and that all individuals give birth independently. Let $Z_n =$
 256 $(I(n), V(n))$ and construct the probability generating function (pgf) for the MTBP,
 257 Z_n .

$$258 \quad \mathbf{F}(\mathbf{u}) = (f_1(\mathbf{u}), f_2(\mathbf{u})) = \left(\frac{\alpha + \delta u_1 u_2 + \bar{S} u_1^2}{\alpha + \delta + \bar{S}}, \frac{\omega + \bar{S} u_1 u_2}{\omega + \bar{S}} \right).$$

259 It follows that Z_n is not singular and the matrix of expectations is given by

$$260 \quad \mathbb{M} = \begin{bmatrix} \frac{\delta + 2\bar{S}}{\alpha + \delta + \bar{S}} & \frac{\delta}{\alpha + \delta + \bar{S}} \\ \frac{\bar{S}}{\omega + \bar{S}} & \frac{\bar{S}}{\omega + \bar{S}} \end{bmatrix},$$

261 is positive. Thus, \mathbb{M} is primitive and Theorem 1 applies. Solving the system of nonlinear
 262 equations given by $\mathbf{F}(\mathbf{q}) = \mathbf{q}$ yields

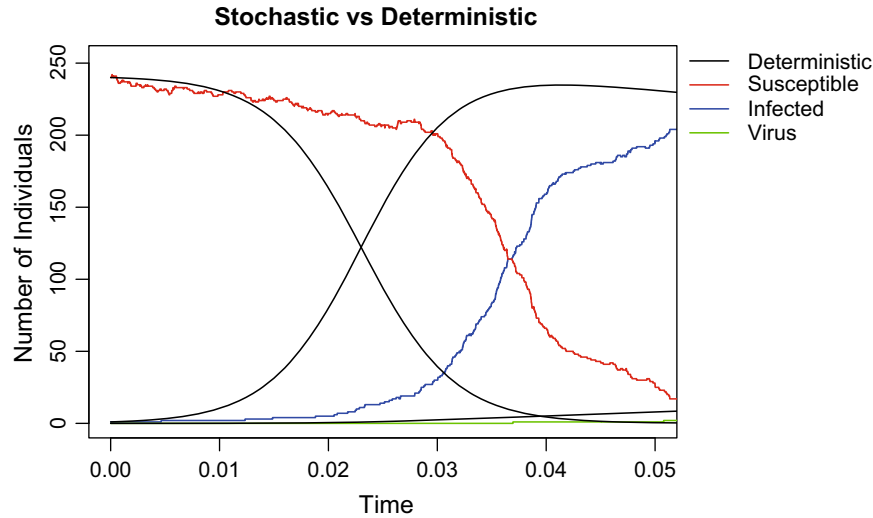


Fig. 1 One realization of the CTMC model, X_t , compared to solution of the deterministic model. Both simulations take initial condition ($S = 240, I = 1, V = 0$) and parameter vector ($\beta = 12, \mu = 0.05, \alpha = 3.3, \delta = 1.3, \omega = 4$)

$$q_1 = \frac{\alpha + \delta + \omega + \bar{S} - \sqrt{(\alpha - (\omega + \bar{S}))^2 + \delta(\delta + 2(\alpha + \omega + \bar{S}))}}{2\bar{S}}, \text{ and} \quad (4)$$

$$q_2 = \frac{\omega}{\omega + \bar{S}(1 - q_1)}. \quad (5)$$

Then the probability of extinction given that $Z_0 = (j_1, j_2)$ is

$$\mathbb{P}_0 = q_1^{j_1} q_2^{j_2}.$$

Note that, for this model, the MTBP approximation of the probability of extinction can be determined analytically. That is, \mathbb{P}_0 can be expressed as a continuous function of the parameters.

3.3 Numerical Example

For the purpose of illustrating the accuracy of the MTBP approximation, we consider the parameter vector given by ($\beta = 4, \mu = 0.05, \alpha = 3.3, \delta = 1.3, \omega = 4$). This choice of parameters yields $\bar{S} = 80$ and $\mathcal{R}_0 \approx 32 \gg 1$. Let \mathbb{P}_0 denote the probability of extinction predicted by the MTBP, given $Z_0 = (I(0), V(0))$. The probability of extinction in the CTMC is estimated by simulating numerically. Let $\mathbb{P}_0^{(1,000,000)}$ denote the probability of extinction approximated by numerical simulation over 1,000,000 realizations. The results of both approximations are presented in Table 4.

Table 4 illustrates that, for this choice of parameters, the MTBP provides extremely accurate results. Since \mathbb{P}_0 can be expressed as a function of the parameters, the computational expense for MTBP approximation is negligible. However, we cannot be certain, a priori, whether or not the disease-free population of susceptible fish is suffi-

Table 4 Probability of extinction of the virus from the initial condition $(\bar{S}, I(0), V(0))$ with the parameter vector $(\beta = 4, \mu = 0.05, \alpha = 3.3, \delta = 1.3, \omega = 4)$ approximated by branching process and numerically over 1,000,000 realizations

$I(0)$	$V(0)$	\mathbb{P}_0	$\mathbb{P}_0^{(1,000,000)}$
1	0	0.0406	0.0407
0	1	0.0495	0.0494
1	1	0.0020	0.0020

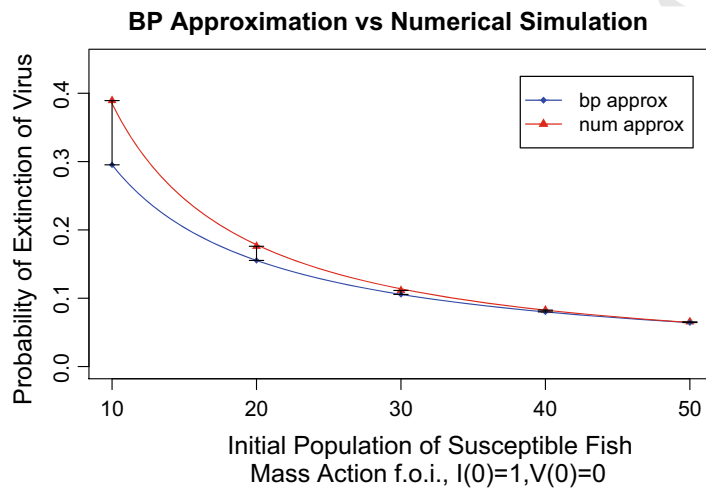


Fig. 2 Comparison of multitype branching process approximation to numerical simulation of probability of extinction in single-patch model with mass action force of infection and high mortality for infected fish

282 ciently large without comparing the MTBP results to numerical simulation. Therefore,
 283 the estimate of computational expense for MTBP approximation should include the
 284 cost of simulating the CTMC. The additional expense for simulating the CTMC can
 285 be significant.

286 In Fig. 2, we compare MTBP and numerical simulation for initial populations at
 287 ten unit increments from 10 to 50. First, note that the population of susceptible fish at
 288 DFE is given by $\bar{S} = \frac{\beta}{\mu}$. Therefore, by assuming $\mu = 1$, we have that $\bar{S} = \beta$. We fix
 289 the remaining parameters ($\mu = 1, \alpha = 3.3, \delta = 1.3, \omega = 4$) and vary β from 10 to
 290 50 in ten unit increments.

291 Numerical data in Fig. 2 are fit with a power law curve $y = bx^\lambda$ where $b = 4.9584$
 292 and $\lambda = -1.11$. Not pictured, the absolute error is fit with a power law curve with
 293 $b = 62.172$ and $\lambda = -2.743$ and the relative error is fit with a power law curve with
 294 $b = 0.4584$ and $\lambda = -0.067$. Since \mathbb{P}_0 is a continuous function of the parameters,
 295 there was no need to fit a curve to the MTBP results.

296 In Sect. 5, we will show that the character and speed of convergence of the MTBP
 297 approximation results to the CTMC simulation results depends on the structure of the
 298 model and the choice of parameters. We do this by constructing illustrations similar
 299 to Figs. 2 and 3 based on variations of the one-patch model.

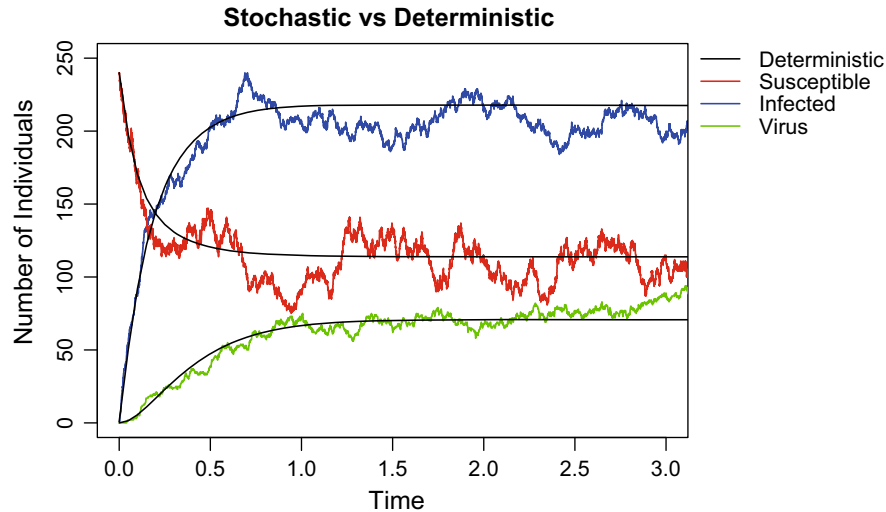


Fig. 3 One realization of the Markov chain model compared to solution of the deterministic model. Both simulations take initial condition ($S = 240, I = 1, V = 0$) and parameter vector ($\beta = 12, \mu = 0.05, \alpha = 3.3, \omega = 4, \delta = 1.3, m_1 = 6, m_2 = 7.5, a_1 = 3, a_2 = 2$)

4 One-Patch Model with Modified Force of Infection

4.1 Deterministic Model

The one-patch model given by system (2) proposes a mass action force of infection. It has been suggested that the f.o.i. may initially be driven by infected salmon encountering susceptible salmon when there are low levels of free virus present at the outset of an exposure event. As more salmon become infected and shed more and more virus into the environment, the free virus may then drive the infection. To account for this, we modify system (2) by considering $f(I, V) = f_2(I, V)$ where

$$f_2(I, V) = \frac{m_1 I}{a_1 + I + V} + \frac{m_2 V}{a_2 + I + V}$$

Note that when $m_1 = m_2$ and $a_1 = a_2$, the growth function $S \left(\frac{m_1 I}{a_1 + I + V} + \frac{m_2 V}{a_2 + I + V} \right)$ simplifies to the standard Michaelis–Menten function for $I + V$. System (2) with $f(I, V) = f_2(I, V)$ admits equilibria at $\mathbf{0}$ and the DFE $(\frac{\beta}{\mu}, 0, 0)$. Following the next generation matrix approach (Diekmann et al. 1990; Driessche and Watmough 2002) the basic reproduction number is determined to be

$$\mathcal{R}_0 = \frac{m_1 a_2 + \frac{\delta}{\omega} m_2 a_1}{\alpha a_1 a_2} \frac{\beta}{\mu}. \quad (6)$$

The endemic equilibrium is a root of the vector field. From $\dot{V} = 0$ we have $V' = \frac{\delta}{\omega} I'$. Substituting into $\dot{I} = 0$ yields $S' = f_1(I')$. Let $f_2(I') = \frac{m_1 I'}{a_1 + (1 + \frac{\delta}{\omega}) I'}$ and $f_3(I') = \frac{m_2 \frac{\delta}{\omega} I'}{a_2 + (1 + \frac{\delta}{\omega}) I'}$. Then the nonnegative root of $\dot{S} = 0$ is a root of the equation

Table 5 State transitions and rates for the CTMC SIV model

Description	Transition	Rate $\sigma(i, j)$
Birth of S	$(S, I, V) \mapsto (S + 1, I, I)$	βS
Death of S	$(S, I, V) \mapsto (S - 1, I, V)$	μS^2
Infection	$(S, I, V) \mapsto (S - 1, I + 1, V)$	$S \left(\frac{m_1 I}{a_1 + I + V} + \frac{m_2 V}{a_2 + I + V} \right)$
Death of I	$(S, I, V) \mapsto (S, I - 1, V)$	αI
Shedding of V	$(S, I, V) \mapsto (S, I, V + 1)$	δI
Clearance of V	$(S, I, V) \mapsto (S, I, V - 1)$	ωV

318
$$\beta - \mu\alpha f_1(I') - f_2(I') - f_3(I') = 0. \tag{7}$$

319 Furthermore, $f_1'(I'), f_2'(I'), f_3'(I') > 0$ and $f_2(0) = f_3(0) = 0$. Thus, (7) has a
 320 unique positive root if and only if $f_1(0) < \beta \iff \mathcal{R}_0 > 1$. Thus, the unique positive
 321 endemic equilibrium exists if and only if $\mathcal{R}_0 > 1$. If $\mathcal{R}_0 \leq 1$, then the DFE is g.a.s..
 322 This system has the same dynamics on the boundary as the system with mass action
 323 f.o.i.. Using arguments similar to those in Milliken (2016), it follows that system (2)
 324 with $f(I, V) = f_2(I, V)$ is uniformly strongly persistent whenever $\mathcal{R}_0 > 1$ (Thieme
 325 1993).

326 **4.2 Stochastic Model**

327 The CTMC model related to system (2) with $f(I, V) = f_2(I, V)$ is characterized by
 328 the transitions and rates given in Table 5.

329 We approximate the CTMC, X_n , near the DFE with the MTBP, Z_n , with the pgf

330
$$\mathbf{F}(\mathbf{u}) = (f_1(\mathbf{u}), f_2(\mathbf{u})) = \left(\frac{\alpha + \delta u_1 u_2 + \bar{S} \frac{m_1}{a_1 + 1} u_1^2}{\alpha + \delta + \bar{S} \frac{m_1}{a_1 + 1}}, \frac{\omega + \bar{S} \frac{m_2}{a_2 + 1} u_1 u_2}{\omega + \bar{S} \frac{m_2}{a_2 + 1}} \right).$$

331 The matrix of expectations is given by

332
$$\mathbb{M} = \begin{bmatrix} \frac{\delta + 2\bar{S} \frac{m_1}{a_1 + 1}}{\alpha + \delta + \bar{S} \frac{m_1}{a_1 + 1}} & \frac{\delta}{\alpha + \delta + \bar{S} \frac{m_1}{a_1 + 1}} \\ \frac{\bar{S} \frac{m_2}{a_2 + 1}}{\omega + \bar{S} \frac{m_2}{a_2 + 1}} & \frac{\bar{S} \frac{m_2}{a_2 + 1}}{\omega + \bar{S} \frac{m_2}{a_2 + 1}} \end{bmatrix}.$$

333 Clearly, the branching process is not singular and \mathbb{M} is a positive matrix. Thus,
 334 Theorem 1 applies. Let $\Delta_1 = \frac{m_1}{a_1 + 1}$, $\Delta_2 = \frac{m_2}{a_2 + 1}$, and

335
$$\mathcal{D} = (\alpha \Delta_2 - \Delta_1 (\bar{S} \Delta_2 + \omega))^2 + \delta \Delta_2^2 (\delta + 2\alpha + 2\bar{S} \Delta_1) + 2\delta \omega \Delta_1 \Delta_2. \tag{8}$$

Table 6 Probability of extinction of the virus from the initial condition (\bar{S}, i_0, v_0) with the parameter vector $(\beta = 4, \mu = 0.05, \alpha = 3.3, \omega = 4, \delta = 1.3, m_1 = 3, m_2 = 2.5, a_1 = 3, a_2 = 2)$ approximated by branching process and numerically over 1,000,000 realizations

$I(0)$	$V(0)$	\mathbb{P}_0	$\mathbb{P}_0^{(1,000,000)}$
1	0	0.0538	0.0548
0	1	0.0596	0.0606
1	1	0.0032	0.0042

336 Then $\mathcal{D} > 0$,

$$337 \quad q_1 = \frac{\alpha \Delta_2 + \delta \Delta_2 + \omega \Delta_1 + \bar{S} \Delta_1 \Delta_2 - \sqrt{\mathcal{D}}}{2\bar{S} \Delta_1 \Delta_2}, \text{ and} \quad (9)$$

$$338 \quad q_2 = \frac{\omega}{\omega + \bar{S} \Delta_2 (1 - q_1)}. \quad (10)$$

340 Given $Z_0 = (j_1, j_2)$, $\mathbb{P}_0 = q_1^{j_1} q_2^{j_2}$ can be expressed as a continuous function of the
341 parameters.

342 4.3 Numerical Example

343 For the purpose of illustrating the accuracy of the MTBP approximation, we consider
344 the parameter vector given by $(\beta = 4, \mu = 0.05, \alpha = 3.3, \omega = 4, \delta = 1.3, m_1 =$
345 $3, m_2 = 2.5, a_1 = 3, a_2 = 2)$. This implies that $\bar{S} = 80$ and $\mathcal{R}_0 \approx 34 \gg 1$. Let \mathbb{P}_0
346 denote the probability of extinction predicted by the MTBP, given $Z_0 = (I(0), V(0))$.
347 The probability of extinction in the CTMC is estimated by simulating numerically. Let
348 $\mathbb{P}_0^{(1,000,000)}$ denote the probability of extinction approximated by numerical simulation
349 over 1,000,000 realizations. The extinction probability predicted by the branching
350 process approximation is compared with numerical results in Table 6.

351 This model represents a variant to the one-patch model studied in Sect. 3 which
352 differs only in the choice of function for the force of infection.

353 5 Critical Size of Disease-Free Population

354 In this section, we illustrate how variations to the underlying model affect the accuracy
355 of MTBP approximation for small initial populations. Figure 2 at the end of Sect. 3
356 shows how MTBP approximation diverges from the probability of extinction in the
357 CTMC for small initial populations when $f(I, V) = f_1(I, V)$. We take this illustration
358 as a baseline and vary the system in two ways. First, we leave $f(I, V) = f_1(I, V)$,
359 but reduce the mortality rate of infected fish from $\alpha = 3.3$ to $\alpha = 1.5$. Second, we
360 let $\alpha = 3.3$ as in the baseline, but let $f(I, V) = f_2(I, V)$ as in the model developed
361 in Sect. 4. In Fig. 4, we set $f(I, V) = f_1(I, V)$ and fix the parameter vector $(\mu =$
362 $1, \alpha = 1.5, \delta = 1.3, \omega = 4)$ with low mortality of infected fish and vary β from 10
363 to 50 in ten unit increments. Numerical data are fit with a power law curve $y = bx^\lambda$

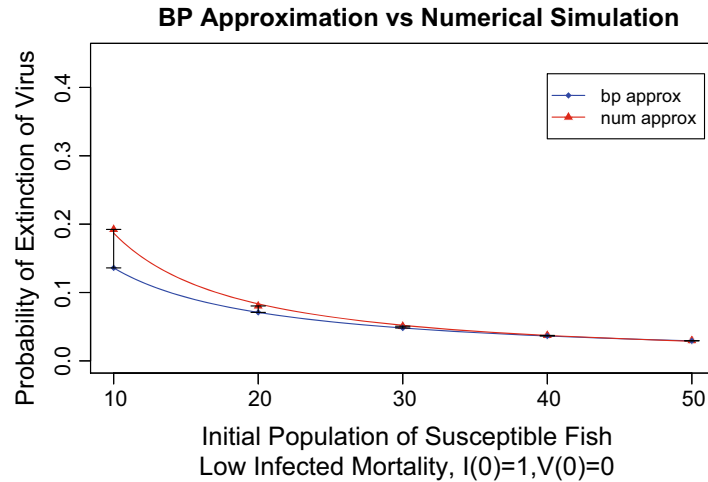


Fig. 4 Comparison of multitype branching process approximation to numerical simulation of probability of extinction in single-patch model with $f(I, V) = f_1(I, V)$ and parameter vector $(\mu = 1, \alpha = 1.5, \delta = 1.3, \omega = 4)$

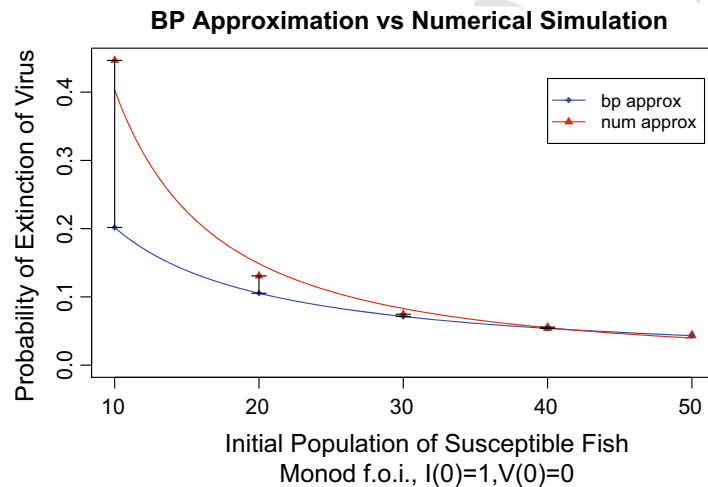


Fig. 5 Comparison of multitype branching process approximation to numerical simulation of probability of extinction in single-patch model with $f(I, V) = f_2(I, V)$ and parameter vector $(\mu = 1, \alpha = 3.3, \delta = 1.3, \omega = 4, m_1 = 6, m_2 = 7.5, a_1 = 3, a_2 = 2)$

364 where $b = 2.7264$ and $\lambda = -1.164$. Not pictured, the absolute error is fit with a power
 365 law curve with $b = 42.109$ and $\lambda = -2.847$ and the relative error is fit with a power
 366 law curve with $b = 14.459$ and $\lambda = -1.659$.

367 In Fig. 5, we set $f(I, V) = f_2(I, V)$ and fix the parameter vector $(\mu = 1, \alpha =$
 368 $3.3, \delta = 1.3, \omega = 4, m_1 = 6, m_2 = 7.5, a_1 = 3, a_2 = 2)$ and vary β from 10 to 50
 369 in ten unit increments. Numerical data is fit with a power law curve $y = bx^\lambda$ where
 370 $b = 11.074$ and $\lambda = -1.439$. Not pictured, the absolute error is fit with a power law
 371 curve with $b = 756.67$ and $\lambda = -3.507$ and the relative error is fit with a power law
 372 curve with $b = 68.329$ and $\lambda = -2.068$.

373 Note that the results in Figs. 2, 4, and 5 are graphed on the same axes on the same
 374 scale. It is immediately evident that the character of convergence of the MTBP varies

Table 7 Entries represent absolute error between numerical results and multitype branching process results, $|\mathbb{P}_0 - \mathbb{P}_0^{(1,000,000)}|$. Column 2 corresponds to Fig. 2, Column 3 to Fig. 4 and Column 4 to Fig. 5

Init. pop.	$f_1, \alpha = 3.3$	$f_1, \alpha = 1.5$	$f_2, \alpha = 3.3$
10	0.094	0.056	0.245
20	0.021	0.009	0.025
30	0.006	0.003	0.003
40	0.003	0.001	0.002
50	0.001	0.000	0.001

375 from the baseline illustration in each of the two latter ones. It is harder to see from the
 376 graphs themselves, but the speed of convergence varies slightly as well. This can be
 377 seen in Table 7.

378 6 Discussion

379 In this article, we use a model of ISAv in two patches and an invariant subsystem
 380 corresponding to one patch as toy models to develop CTMC models and MTBP
 381 approximations to estimate the probability of disease outbreak. In addition to these
 382 models, we formulate a new one-patch model by varying the force of infection func-
 383 tion. In the case of the two-patch model, we approximate the probability of disease
 384 extinction, \mathbb{P}_0 , by iterating the probability generating function of the MTBP. For each
 385 one-patch model, characterized by its force of infection, it is possible to write the
 386 MTBP approximation of \mathbb{P}_0 as a continuous function of the parameters. By compar-
 387 ing MTBP results to numerical simulation of the related CTMC, we show that, for
 388 large initial populations of susceptible fish, the MTBP approximation provides a good
 389 estimate of \mathbb{P}_0 . However, we should also note that MTBP approximation fails to pro-
 390 vide accurate estimates of \mathbb{P}_0 when the initial population of susceptible fish is low.
 391 It is therefore necessary to approximate \mathbb{P}_0 by numerical simulation concurrent with
 392 MTBP approximation. While the computational expense for MTBP approximation is
 393 negligible, the computational expense for numerical simulation of the related CTMC,
 394 can be very high, especially for metapopulation models.

395 In this article, we have not provided an analytical estimate on how large the initial
 396 population of susceptible individuals needs to be in order for the MTBP approximation
 397 to provide a good estimate of \mathbb{P}_0 . We have, however, illustrated the manner in which
 398 the approximation diverges from the true probability in several test cases. Comparison
 399 of results in Figs. 2, 4, 5 and Table 7 suggests that an analytical estimate will be model
 400 specific and parameter dependent.

401 In Whittle (1955), Whittle determined that the probability of extinction for a
 402 susceptible–infected (SI) model was the reciprocal of \mathcal{R}_0 . This result was also ver-
 403 ified by Allen and Lahodny (2012). Allen and Driessche (2013) showed that $1 - \sigma$
 404 and $1 - \mathcal{R}_0$ have the same sign, where σ is the spectral radius of the matrix of first
 405 moments, \mathbb{M} . This implies that efforts that reduce \mathcal{R}_0 will also increase the probabil-
 406 ity of extinction. For the models studied in this article, one way to reduce \mathcal{R}_0 is to
 407 decrease the birth rate of susceptible fish, β . Unfortunately, this also has the effect of
 408 reducing the disease-free equilibrium population size. Nevertheless, in Figs. 2, 4 and

5, we see that as β is decreased, the probability of extinction increases as measured both by branching process approximation and computer simulation.

Metapopulation models are characterized by their patch structure and the rates of migration between patches. In order to study stochastic metapopulations, it would be useful to study how statistics like probability of extinction vary from patch to patch. In addition, the probability of partial extinction events, like extinction in one patch, may be useful in measuring the effectiveness of control strategies. One would expect it to be especially useful when studying the effectiveness of control strategies that are deployed heterogeneously. Mathematically, the problem of calculating the probability of extinction corresponds to the classical problem of hitting a subspace of the state space of the CTMC from some initial state. In the case of total extinction events, this relates to hitting the subspace of the state space where all infectious classes are zero. Taking the two-patch model (1) as an example, total disease extinction relates to hitting the subspace $\{S_1, S_2 \geq 0, I_1 = I_2 = V_1 = V_2 = 0\}$. However, for partial extinction events, it relates to hitting a subspace of the state space where some infectious classes are zero, but others are positive. For example, extinction in patch one of the two-patch model relates to hitting the subspace $\{S_1, S_2 \geq 0, I_2, V_2 > 0, I_1 = V_1 = 0\}$. MTBPs track only the infectious classes and are constructed to calculate the probability of hitting the origin, $\mathbf{0}$. As such, MTBP approximation is only suited to calculating the probability of total extinction.

Acknowledgements This work was conducted with the support from NSF Grants DMS-1411853, DMS-1515661 and the Center for Applied Mathematics at University of Florida. The author would like to thank the referees for their helpful suggestions.

References

- Allen LJS (2003) An introduction to stochastic process with applications to biology. Pearson/Prentice Hall, Upper Saddle River
- Allen LJS, Lahodny GE (2012) Extinction thresholds in deterministic and stochastic epidemic models. *J Biol Dyn* 6(2):590–611
- Allen LJS, Lahodny GE (2013) Probability of a disease outbreak in stochastic multipatch epidemic models. *Bull Math Biol* 75(7):1157–1180
- Allen LJS, van den Driessche P (2013) Relations between deterministic and stochastic thresholds for disease extinction in continuous- and discrete-time infectious disease models. *Math Biosci* 243(1):99–108
- Ball FG (1983) The threshold behaviour of epidemic models. *J Appl Prob* 20(7):227–241
- Ball FG, Donnelly D (1995) Strong approximations for epidemic models. *Stoch Proc Appl* 55(1):1–21
- Beretta E, Kuang Y (1998) Modeling and analysis of a marine bacteriophage infection. *Math Biosci* 149:57–76
- Britton T (2010) Stochastic epidemic models: a survey. *Math Biosci* 225:24–35
- Butler G, Freedman HI, Waltman P (1986) Uniformly persistent systems. *Proc Am Math Soc* 96:425–430
- Diekmann O, Heesterbeek JAP, Metz JAJ (1990) On the definition and computation of the basic reproduction ratio R_0 in models of infectious disease in heterogeneous populations. *J Math Biol* 28:365–382
- Dorman KS, Sinsheimer JS, Lange K (2004) In the garden of branching processes. *SIAM Rev* 46(2):202–229
- Falk K, Namork E, Rimstad E, Mjaaland S, Dannevig BH (1997) Characterization of infectious salmon anemia virus, an Orthomyxo-like virus isolated from Atlantic salmon (*Salmo salar* L.). *J Virol* 71(12):9016–23
- Fonda A (1988) Uniformly persistent semidynamical systems. *Proc Am Math Soc* 104:111–116
- Freedman HI, Ruan S, Tang M (1994) Uniform persistence and flows near a closed positively invariant set. *J Dyn Differ Equ* 6(4):583–600
- Garay B (1989) Uniform persistence and chain recurrence. *J Math Anal Appl* 139:372–381

- 457 Griffiths M, Greenhalgh D (2011) The probability of extinction in a bovine respiratory syncytial virus
458 epidemic model. *Math Biosci* 231(2):144–158
- 459 Harris TE (1963) *The theory of branching processes*. Springer, Berlin
- 460 Hofbauer J, So JW-H (1989) Uniform persistence and repellers for maps. *Proc Am Math Soc* 107(4):1137–
461 1142
- 462 Kimmel M, Axelrod DE (2002) *Branching processes in biology*. Springer, New York
- 463 Mardones FO, Perez AM, Carpenter TE (2009) Epidemiologic investigation of the re-emergence of infec-
464 tious salmon anemia virus in Chile. *Dis Aquat Org* 84(2):105–14
- 465 Milliken E, Pilyugin SS (2016) A model of infectious salmon anemia virus with viral diffusion between
466 wild and farmed patches. *DCDS-B*, Accepted
- 467 Mode CJ (1971) *Multitype branching processes theory and applications*. Elsevier, New York
- 468 Nowak MA, May RM (2000) *Virus dynamics*. Oxford University Press, New York
- 469 Perelson AS, Nelson PW (1999) Mathematical analysis of HIV-I: dynamics in vivo. *SIAM Rev* 41(1):3–44
- 470 Seneta E (1998) *IJ Bieneymé [1796-1878]: criticality, inequality and internationalization*. *Int Stat Rev*
471 66(3):291–301
- 472 Thieme HR (1993) Persistence under relaxed point dissipativity (with applications to an endemic model).
473 *SIAM J Math Anal* 24(2):407–435
- 474 Van Den Driessche P, Watmough J (2002) Reproduction numbers and sub-threshold endemic equilibria for
475 compartmental models of disease transmission. *Math Biosci* 180:29–48
- 476 Vike S, Nylund S, Nylund A (2009) ISA virus in Chile: evidence of vertical transmission. *Arch Virol*
477 154(1):1–8
- 478 Watson HW, Galton F (1875) On the probability of the extinction of families. *J Anthropol Inst Gt Britain*
479 *Irel* 4:138–144
- 480 Whittle P (1955) The outcome of a stochastic epidemic- a note on Bailey's paper. *Biometrika* 42:116–122

Journal: 11538
Article: 355

Author Query Form

**Please ensure you fill out your response to the queries raised below
and return this form along with your corrections**

Dear Author

During the process of typesetting your article, the following queries have arisen. Please check your typeset proof carefully against the queries listed below and mark the necessary changes either directly on the proof/online grid or in the 'Author's response' area provided below

Query	Details required	Author's response
1.	Kindly check and confirm corresponding author mail id is correctly identified.	
2.	Kindly check and confirm inserted city, state and country is correctly identified for the affiliation.	
3.	Please provide minimum 3–6 keywords.	
4.	Please check and confirm if the inserted citation of Figs. 1 and 3 are correct. If not, please suggest an alternate citation. Please note that figures and tables should be cited sequentially in the text.	